Available online at www.sciencedirect.com
ScienceDirect
Polymer 47 (2006) 6731–6737
polymer
www.elsevier.com/locate/polymer

Non-linear shear deformation of hydrophobically modified polyelectrolyte systems

K.C. Tam [a,*], W.K. Ng [a], R.D. Jenkins [b]

[a] School of Mechanical and Aerospace Engineering, Nanyang Technological University, 50 Nanyang Avenue, Singapore 639798, Singapore
[b] The Dow Chemical Company, UCAR Emulsion Systems, 410 Gregson Drive, Cary, NC 27511, USA

Received 16 April 2006; received in revised form 4 July 2006; accepted 23 July 2006
Available online 9 August 2006

Abstract

The shear imposed oscillation technique was employed to probe the shear-induced structural changes of 3 wt% hydrophobically modified polyelectrolyte solutions that possess shear-thinning and shear-thickening behavior. The shear-thickening behavior is related to the transformation of predominantly intra-molecular to inter-molecular associations. On the other hand, the shear-thinning behavior under moderate shear deformation is caused by the re-organization of the transient network structure. Under high shear deformation, the shear-thinning behavior is solely caused by the shear-induced effect that increases the chain-end exit rate, which reduces the mechanically active chains and lifetime of the hydrophobe in the micellar junctions.

Keywords: Associative polymers; Rheology; Non-linear viscoelasticity

1. Introduction

Hydrophobically modified alkali-soluble emulsion (HASE) polymers have received considerable attention in recent years [1–12]. This class of hydrophobically modified anionic polyelectrolyte system is prepared by emulsion polymerization at low pH to yield an acid-rich co-polymer in the form of a dispersion of latex particles. Each particle may contain as many as 10–50 polymer chains. When a base is added to the dispersion, the −COOH groups of the polymer are neutralized. The particles swell and dissolve, releasing charged polymeric chains into the solution [12]. The polymer solution thickens by an associative mechanism (intra- or inter-molecular) and by the expansion of the high-molecular-weight polymer backbone [7,10]. The creation of the polymer network commences when the hydrophobes attached to its polymer backbone begin to associate, which produces a network structure consisting of numerous polymeric chains.

The grafting of hydrophobic groups to the water-soluble polymer backbone enhances the rheological properties when compared to those without hydrophobic groups. The increase in the viscosity profile is caused by the self-association of the hydrophobic groups, yielding inter-molecular networks in solution [11,13–17]. Volpert et al. [18] and Aubry and Moan [19] observed lower rheological properties for the modified hydrophobic system at low polymer concentrations. They attributed this behavior to the formation of intra-molecular associations between the hydrophobes along the same polymer chain. As a result, the dimension of the polymer coil is reduced, yielding a lower radius of gyration that corresponds to a lower viscosity.

The structure of the associative polymer with hydrophobes attached as pendant side chain is much more complex when compared to end-capped hydrophobic systems. This is due to the steric hindrance of the polymer backbone that prevents the formation of hydrophobic junctions, yielding hydrophobic junctions/clusters with a poly-dispersed aggregation number [8,14,20–23]. On the other hand, the comb-type polymer exhibits a better viscosity enhancement than the end-capped

* Corresponding author. Fax: +65 67911859.
E-mail address: mkctam@ntu.edu.sg (K.C. Tam).

0032-3861/$ - see front matter © 2006 Elsevier Ltd. All rights reserved.
doi:10.1016/j.polymer.2006.07.051

system [21,24]. This is because the combed system is more efficient in creating bridges between micelles, yielding larger number of inter-molecular associative junctions compared to HEUR system. Moreover, the rheological properties of the associative polymer can be further enhanced by the extension of the branched alkyl chain and by increasing the hydrophobicity of the hydrophobic moieties [20,25–27]. This will slow down the dynamic exchange rate between the micellar junctions, which increases the relaxation time of the polymer system. Leibler et al. [28] presented a relaxation model of a polymer system with reversible network, where the relaxation behavior was divided into two different processes. The slower process is related to the reptation motion of polymer chains by coherent breaking of a few cross-links at a time, which is dependent on the degree of association, while the faster process is due to the relaxation of segments between entanglement points and related to the average lifetime of the association.

As a result of the hydrophobic side chain, which gives rise to multiple relaxation times, the polymer system can no longer be described by a single Maxwell model. Therefore, the prediction of the lifetime of the polymer using the dynamic cross-over frequency and onset of steady rate viscosity may not be applicable [19]. Alternative technique for determining the characteristic lifetimes of the comb polymer is to measure N_1 (first Normal stress) at low shear [21] and the relaxation time was calculated to be $\sim$0.01 s. Recent studies by Tirtaatmadja et al. [20] and Seng et al. [29] showed that with the addition of non-ionic surfactant, a sharp discontinuity in viscosity was observed at high shear stresses. The shear-thickening behavior observed is commonly due to (i) the stretching of elastic polymeric segments beyond its linear viscoelastic region [1], (ii) a change from intra-molecular to inter-molecular hydrophobic association brought about by the unfolding of polymer chains at high shear rates [2,18,29], (iii) dangling segments being recaptured by the network before they have the opportunity to fully relax to the equilibrium state [10,30]. The shear-thinning is generally believed to be caused by shear-induced disruption of the network formed by the weak associating hydrophobic groups.

The viscoelasticity of the polymer can be differentiated into two regions, linear and non-linear viscoelastic regions. On application of a small strain, $\gamma < \gamma_c$, the relaxation modulus will collapse onto a master curve indicating linear viscoelastic behavior. Often, the master curve may be obtained by shifting the horizontal and vertical axes. As the applied strain is larger than the critical strain, $\gamma > \gamma_c$, the relaxation modulus is no longer independent of strain yielding the non-linear viscoelastic behavior. If the stress relaxation modulus in the non-linear behavior is parallel to those in the linear viscoelastic region, it means that the time dependence of $\tau(\gamma,t)$ is factorable from the strain dependence [31,32],

$$\tau(\gamma,t) = G_o(t)h(\gamma)\gamma$$

$$G(\gamma,t) = G_o(t)h(\gamma) \quad (1)$$

where $h(\gamma)$ is the damping coefficient (shift factor) at strain γ, $G_o(t)$ is the relaxation modulus in linear viscoelastic region.

The structural behaviors of the associative polymers under the application of shear and strain deformations were investigated using the superposition of oscillation on steady shear flow and stress relaxation. Such information provides insights into the structure under deformation that is relevant to many processes. The polymer systems used are 3 wt% HASE05-20 and HASE40-20. These polymers were chosen because they exhibit different shear deformation behaviors. HASE05-20 exhibits a continuous shear-thinning behavior while HASE40-20 possesses shear-thickening behavior at moderate shear rate.

2. Experimental

The model associative polymers studied are hydrophobically modified, alkali-soluble (HASE) polymers synthesized by Dow Chemicals (formerly Union Carbide), via the emulsion polymerization of methacrylic acid (MAA), ethyl acrylate (EA) and a macromonomer that had been capped with a hydrophobic group. The polymer examined in the present work has a chemical structure shown in Fig. 1, where R is C_nH_{2n+1} alkyl chain, and the ratio of x:y:z in mol% is 50:49:1.

The polymer examined is designated as HASE05-20 and HASE40-20, where the ethylene-oxide spacer chain length of HASE40-20 is 40 mol while HASE05-20 is 5 mol. The hydrophobes of the polymers consist of the $C_{20}H_{41}$ alkyl chain. A brief description of the synthetic route of the model polymer has been previously reported [1,3] and will not be presented here. It has an average molecular weight of approximately 200,000–250,000 g/mol determined by intrinsic viscosity [2] and static light scattering measurements [33,34]. The molecular weight and monomer sequence distribution of these polymers are believed to be quite similar since the process used to produce them was held constant [34]. Recently, Sprong and co-workers synthesized HASE polymers with well-controlled molar masses and narrow molar mass distributions using the reversible addition–fragmentation chain transfer

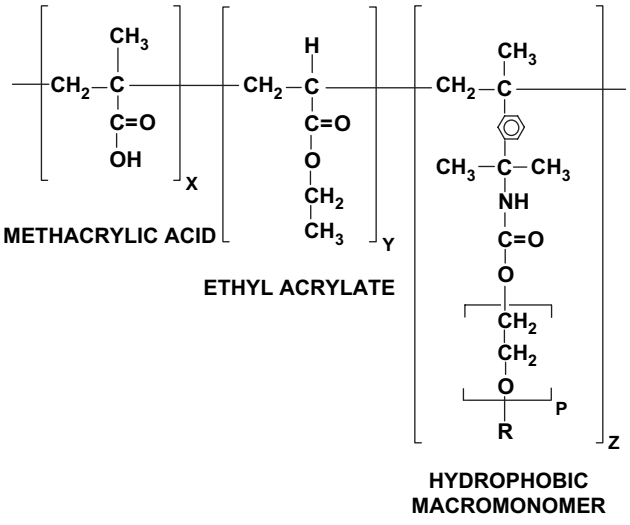

Fig. 1. Chemical structure of model HASE polymers.

polymerization of methyl methacrylate and methacrylic acid. Molecular weights ranging from 27,000 to 50,000 g/mol with polydispersity index of 1.2–1.5 were reported [35].

The samples of desired concentrations were prepared from a stock solution of 3 wt% polymer in 10^{-4} M KCl by diluting with 10^{-4} M KCl solution. The alkaline used to neutralize the polymer to the required pH of 9.0 is 2-aminomethylpropanol (AMP). This is to ensure complete neutralization of the polymer where maximum enhancement of the rheological properties was observed [7].

Two rheometers were used to measure the shear and strain properties of the associative polymer systems. Superposition of oscillation on shear technique was employed using the Controlled Stress Carr-Med CSL500 rheometer for determining the structural behavior at various stages of applied stresses. The geometry used with the CSL500 is a cone and plate system with diameter 40 mm and 2° cone angle. The stress relaxation modulus was measured using the ARES rheometer with a similar cone and plate system but with a cone angle of 2.3°.

3. Results and discussion

The structural properties of associative polymers, which possess shear-thickening and shear-thinning or combination of both behaviors under shear deformation were investigated. In order to obtain detailed structural information, the superposition of oscillation on shear technique was employed [8,20,23]. A shear stress was applied for a fixed time to achieve an equilibrium condition. Once the equilibrium condition was achieved, a superimposed oscillation was applied to probe the viscoelastic behavior of the solution at that condition. Using this technique, the viscoelastic response of large network elements and fast response of the dynamic cluster under different applied stresses can be determined from the relaxation time spectrum. In addition to the parallel superposition technique [20], non-linear shear deformation over a wide deformation regime was examined, and the molecular and bulk properties over a wide deformation regime were elucidated.

The dynamic properties of 3 wt% HASE05-20 and HASE40-20 are plotted in Fig. 2a and b, respectively. Upon the application of stresses, the terminal region shifts to higher frequencies. The dynamic data of 3 wt% HASE40-20 at applied stress of 0, 50 and 100 Pa were fitted with the multiple modes Maxwell model (Fig. 3a–c), where the solid lines represent the best fit for the Maxwell model shown below:

$$G'(\omega) = \sum_{i=1}^{N} \frac{G_i \omega_i^2 \lambda_i^2}{1 + \omega_i^2 \lambda_i^2}$$

$$G''(\omega) = \sum_{i=1}^{N} \frac{G_i \omega_i \lambda_i}{1 + \omega_i^2 \lambda_i^2} \quad (2)$$

where "N" is the number of modes in the Maxwell equation. Good fits to the data are observed for conditions of zero or low applied stresses for N ranging from 3 to 4. However, at higher stresses, where the viscosity begins to decrease significantly,

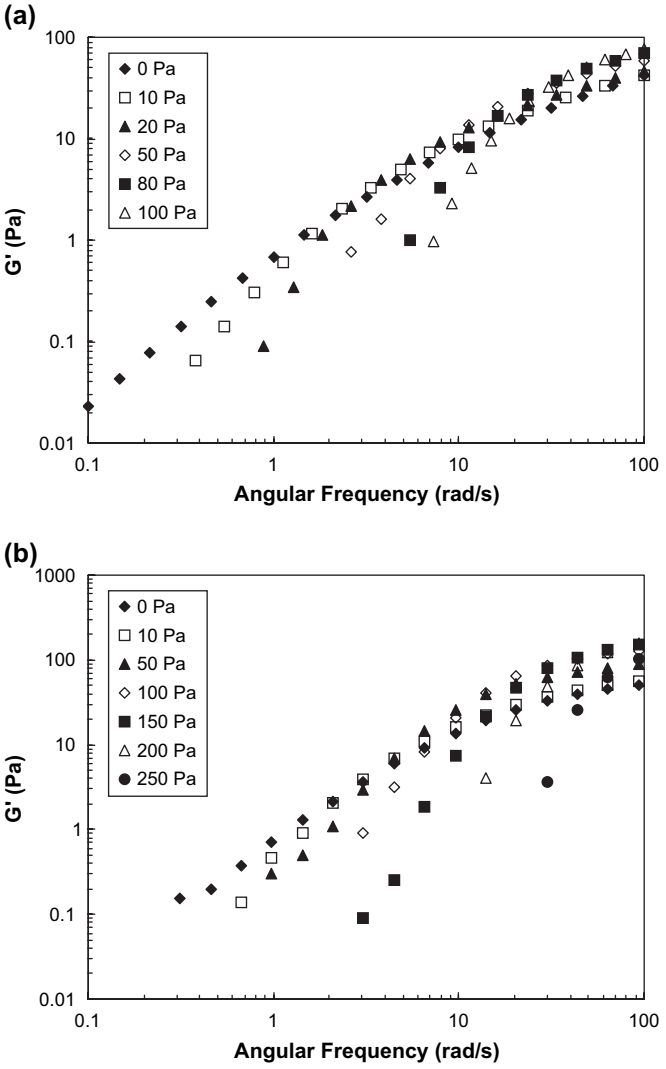

Fig. 2. Linear viscoelastic properties of (a) 3 wt% HASE05-20 at applied stress of 0–100 Pa; (b) 3 wt% HASE40-20 at applied stress of 0–250 Pa.

the Maxwell model is less able to describe the viscoelastic behavior of the solution. This is probably due to the non-linear nature of the coupled deformation in the parallel superposition technique. In order to ensure that the dynamic data at different shear stresses reflect the true material properties, the oscillatory steady shear viscosity was then compared with the equilibrium shear viscosity. The comparison showed that the viscosities are fairly identical, after taken into account the experimental errors, which gives us the confidence that the dynamic frequency sweep data can be used to describe the structural behavior of the polymer systems using the transformed relaxation time spectrum. It is to be noted that in addition to parallel superposition, orthogonal superposition can also be used to study the micro-structural evolution of the material under shear. Vermant et al. reported recently a comparison between both techniques and concluded that orthogonal superposition can be related more directly to the microstructure than the parallel superposition technique [36]. They also showed that the experimental values of the moduli obtained from the parallel and orthogonal superposition measurements

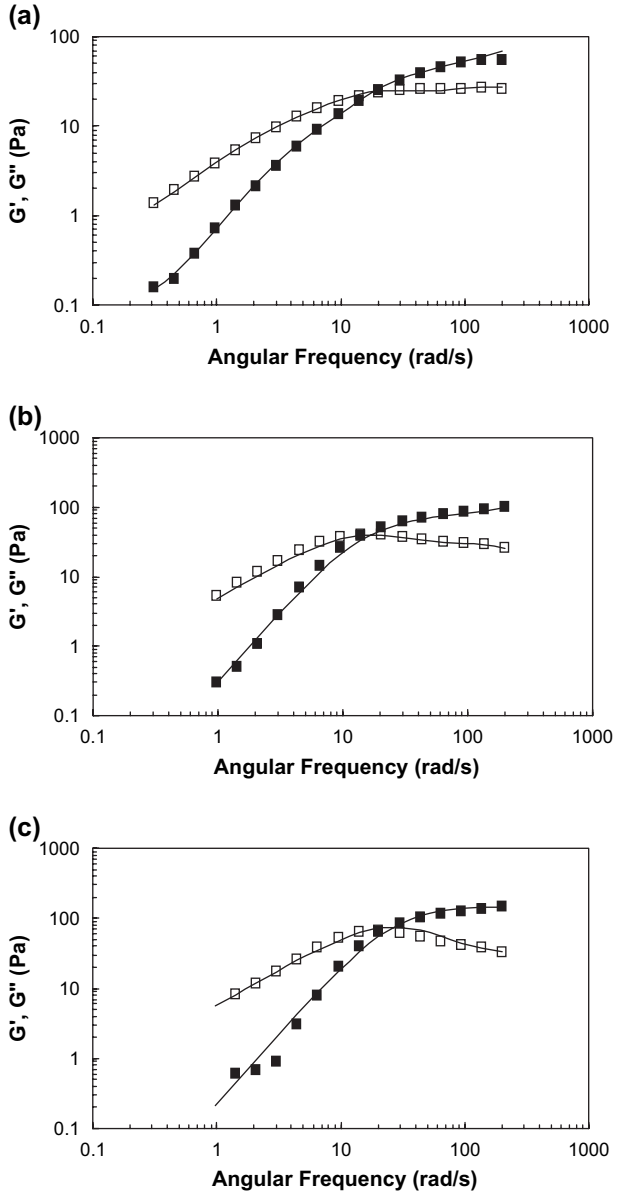

Fig. 3. Fitting of Maxwell model to the dynamic properties of 3 wt% HASE40-20 at (a) 0 Pa; (b) 50 Pa; (c) 100 Pa; loss modulus (□); storage modulus (■).

were related to each other as derived using the K-BKZ model. Despite the fact that the main and the imposed parallel shear fields are coupled for parallel superposition measurement, qualitative information on the structural evolution under shear can be inferred from such studies. For the cases where no terminal region is detected within the experimental frequency range, the relaxation time is taken to be the inverse of the frequency at the point of interception between the curves.

The shear-thinning behavior upon the application of shear stress exhibited by most HASE polymer system, except HASE40-20, is believed to be related to the curtailing of the longest relaxation time [20]. In order to have a clearer picture on the structural behavior of the polymer systems under shear deformation, the 3 wt% HASE05-20 was subjected to parallel superposition oscillation experiments. At the applied stresses of 5–100 Pa, the storage modulus, thus the mechanically active junction densities of the polymer system increased with the application of the shear stress (Fig. 4a). However, the strength of the network structure based on the activation energy plot (derived from the slope of log (η_o) versus $1/T$ according to Arrhenius equation) [17], remains constant over this range of applied stresses (Fig. 4c). The strength of the network is defined as the strength of each hydrophobic junction multiplied by the number of mechanically active junction within the network [29]. Therefore, the decrease in the network strength caused by the reduction in relaxation time (Fig. 4b) is compensated by the increase in junction densities (Fig. 4a), leading to a constant activation enthalpy in this range of applied stresses.

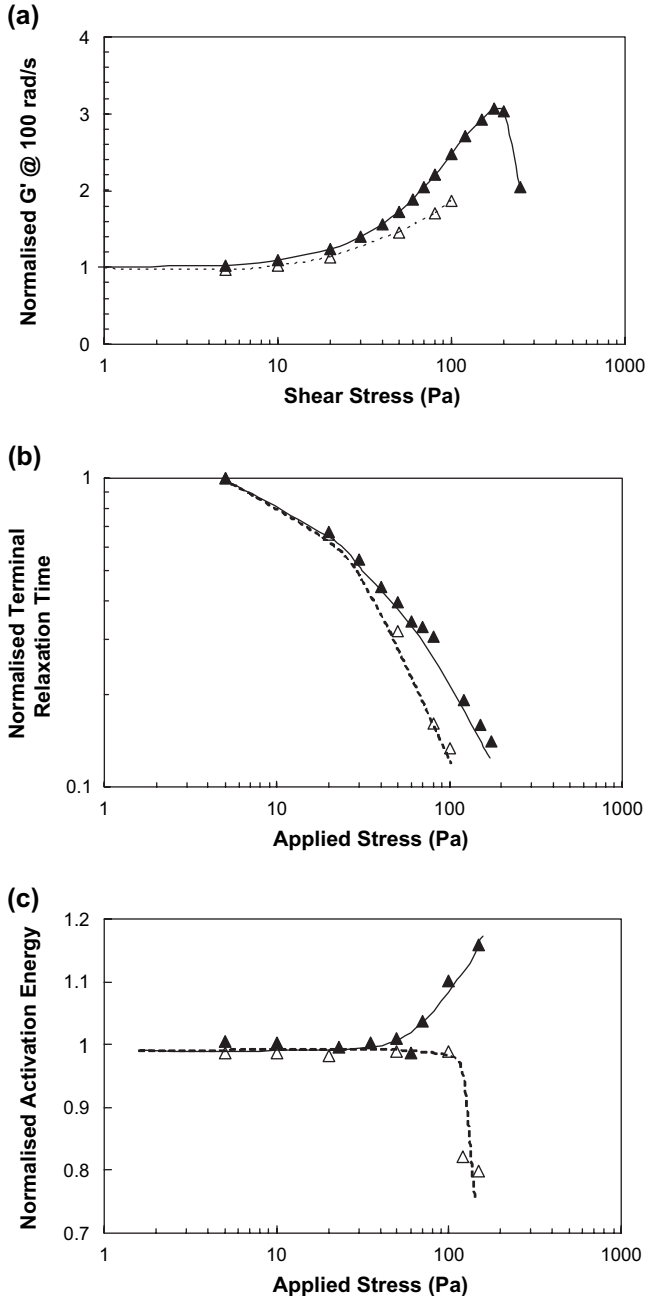

Fig. 4. Normalised rheological properties of 3 wt% solutions: (a) storage modulus at 100 rad/s; (b) average terminal relaxation time; (c) activation energy; HASE05-20 (open symbol); HASE40-20 (closed symbol).

Beyond the shear stress of 100 Pa, where the viscosity decreases sharply, the activation energy of the polymer system exhibits a large drop. The reduction in the strength of the network is mainly attributed to the loss of network connectivity and the reduction in lifetime of the junction. Hence, it is expected that the storage modulus and average terminal relaxation time will decrease accordingly. However, due to the sensitivity and limitation of the equipment, the dynamic data above 100 Pa could not be measured.

The shear-thickening behavior in HASE40-20 warrants further discussion here. This shear-thickening property has been attributed to the transformation of intra- to inter-molecular association. The dynamic properties of HASE40-20 at different applied stresses were measured to clarify the mechanism derived from previous studies [10,23]. Fig. 4a reveals that as the applied stress increased from 5 to 175 Pa, the junction densities in the network increased continuously. However, the strength of the network as indicated by the activation energy remained constant until an applied stress of 60 Pa. It then increases significantly over the shear-thickening region. On the other hand, the overall relaxation time of the polymer system shown in Fig. 4b displays the same behavior as HASE05-20, where it decreases with applied stresses. What then is the cause for the increase in the activation energy and shear-thickening behavior observed in the 3 wt% HASE40-20, which is not present in the HASE05-20 system? By comparing the normalized storage modulus and viscosity-based activation energy in Fig. 4a and c, it is evident that the increase in the junction densities and activation energies with applied stress for HASE40-20 are higher. In addition, the normalized relaxation time plot (Fig. 4b) demonstrates that HASE40-20 possesses a greater resistance to shear deformation as depicted by the slower decrease in the relaxation time compared to HASE05-20. The above observations clearly show that the increase in the strength of the network in the shear-thickening region is caused by the formation of greater number of active junctions in the network. One would then ask as to "where do these additional junction densities come from?" One probable source of the additional junction densities is the conversion of intra- to inter-molecular associations. As HASE40-20 possesses the longest ethylene-oxide spacer chain (40 mol) compared to HASE05-20, the probability of intra-molecular interaction is the highest since the hydrophobes can extend to a greater distant and associate with other hydrophobes on the same polymer chain. The formation of larger number of intra-molecular association in the network causes the polymer to coil into a more compact conformation. Upon the application of stress, the polymer backbones unfold, and this process fragments the intra-molecular junctions, making available greater number of "free" or unassociated hydrophobes which can then form inter-molecular junctions with other hydrophobes in solution. The net result is the apparent increase in the network junction density, which contributes to the strength of the network structure. Above an applied stress of 175 Pa, the drastic reduction in the rheological properties is mainly due to the loss of network connectivity and reduction in lifetime of the structure.

In order to obtain a deeper understanding on the structural property of HASE polymeric systems under shear deformation, the relaxation behaviors were investigated by examining the relaxation spectra as shown in Fig. 5a and b for 3 wt% HASE05-20 and HASE40-20, respectively. The relaxation spectrum $H(\lambda)$ can be derived by transforming the storage and loss moduli in the frequency domain according to the expressions below [37]:

$$G'(\omega) = \int_{-\infty}^{\infty} H(\lambda)\left[\frac{\omega^2\lambda^2}{1+\omega^2\lambda^2}\right] \mathrm{d}(\ln\lambda)$$

$$G''(\omega) = \int_{-\infty}^{\infty} H(\lambda)\left[\frac{\omega\lambda}{1+\omega^2\lambda^2}\right] \mathrm{d}(\ln\lambda) \tag{3}$$

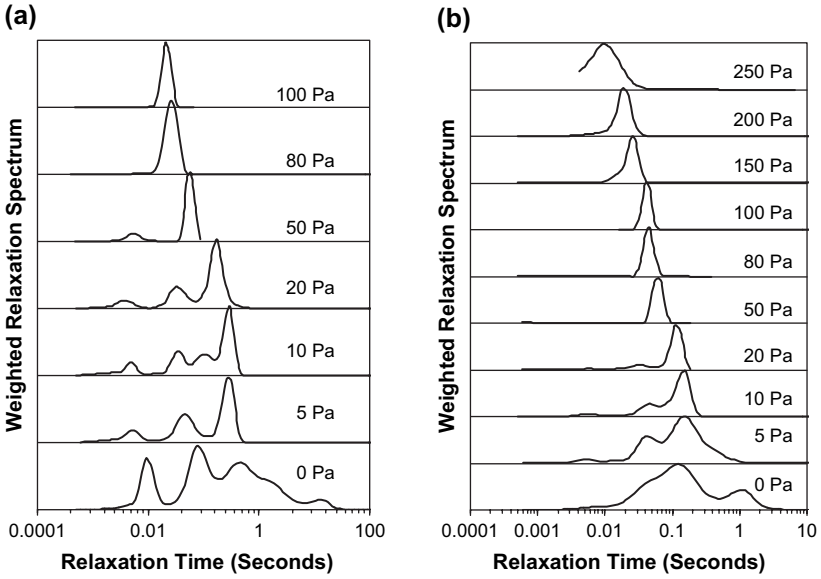

Fig. 5. Weighted relaxation spectrum of 3 wt% solutions at varying applied stresses: (a) HASE05-20; (b) HASE40-20.

The relaxation time spectrum was mathematically computed using a commercial software based on the inverse Laplace algorithm provided by Rheometric Scientific Inc. (Orchestrator software).

Upon the application of shear deformation, the width of the relaxation time spectrum decreases and the relaxation peaks shift to shorter times. However, due to limitation of the equipment, the relaxation time of less than 0.01 s cannot be measured. It is evident that at lower shear deformation, the lifetime of the polymer system continues to decrease with increasing applied stress. The reduction in the lifetime, as represented by the fast peak, indicates that the long relaxation time connected to the junctions with high aggregation number is disrupted. This disruption leads to the re-organization of the network structure, which has the effect of narrowing the distribution of the aggregation number in the associating junctions. The net result is the overall reduction in both the lifetime and the structural relaxation time of the polymer network. In addition, free hydrophobes from the disrupted junctions re-associate to form junctions with lower aggregation number, which raises the number of mechanically active junctions in the polymer network (Fig. 4a). Deformation of the HASE polymer at higher stresses results in the overall reduction of junction densities, junction strength, lifetime and relaxation time of the system. This behavior corresponds to the transient network theory proposed by Tanaka and Edwards [38]. They stated that the exit rate of the hydrophobe depends on the applied stress, which is enhanced by the application of stress. This indicates that the applied stress is sufficiently high to reduce the lifetime of the micellar junction. Hence, the drastic reduction in the viscosity profile observed for both polymeric systems is caused by the increase in the chain-end exit rate due to applied stress.

The dynamic strain sweep experiments were conducted to determine the range of linear viscoelastic behavior prior to the selection of the applied strain for the frequency sweep experiments. Strain-thickening behavior is observed for all the HASE polymer systems as shown in Fig. 6a, but the thickening behavior is not observed in the shear viscosity plot (with the exception of HASE40-20). This behavior was also documented by Tirtaatmadja et al. [20] and Tam et al. [10]. The stark contrast between the shear and oscillating strain deformation reveals that the rheological behavior of these polymer solutions is probably due to the reverse flow in the dynamic strain deformation.

In order to verify the above hypothesis, two polymer systems, 3 wt% HASE05-20 and HASE40-20 were subjected to dynamic strain and double step-strain/stress relaxation experiments [39]. The double step-strain experiments were conducted by subjecting the polymer to a positive strain (30 s clockwise step-strain) followed by an instantaneous strain in the reverse direction for 30 s ($\gamma_1 = -\gamma_2$). The main purpose of this experiment is to identify possible recovery of the structure of the polymer systems that undergo reverse flow at different applied strains. The strain profiles of the HASE polymer systems conducted under dynamic strain and double step-strain experiments are plotted in Fig. 6b and c, respectively. The strain profiles were determined from the relaxation modulus in each direction (clockwise and counter-clockwise step-strain) using Eq. (1).

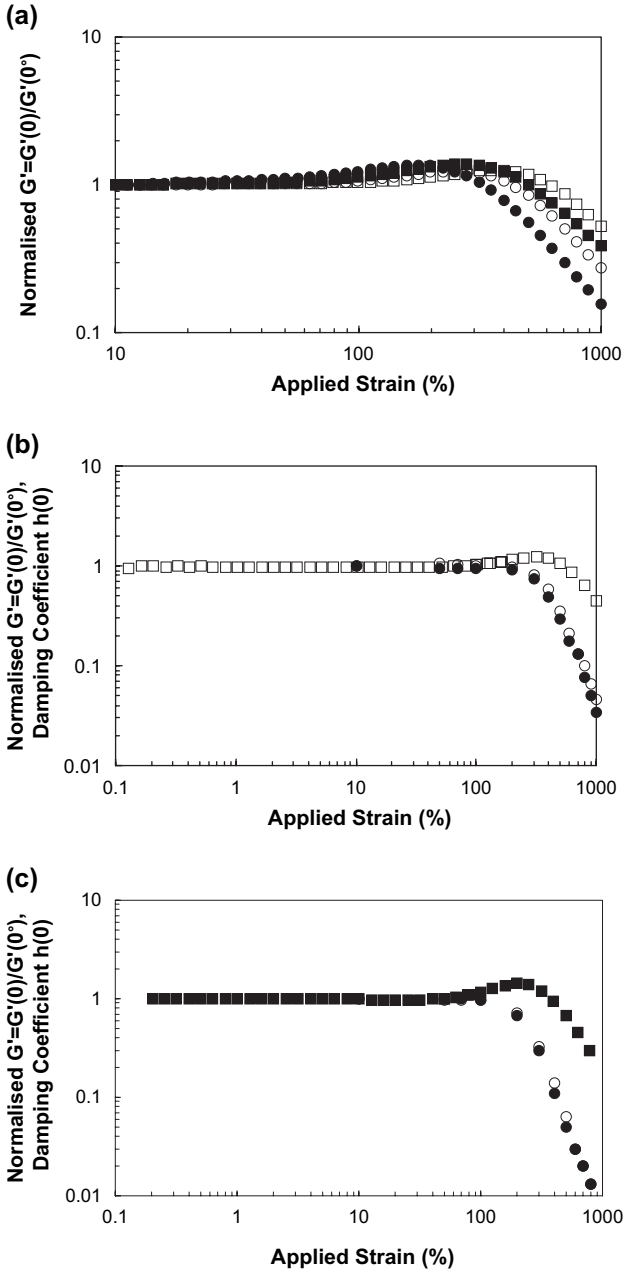

Fig. 6. (a) Dynamic strain sweep of 3 wt% solution at 10 rad/s: HASE05-20 (□), HASE15-20 (○), HASE25-20 (●), HASE40-20 (■); (b) damping coefficient as a function of strain for 3 wt% HASE05-20: normalized G' (□), clockwise damping coefficient (○), counter-clockwise damping coefficient (●); (c) damping coefficient as a function of strain for 3 wt% HASE40-20 normalized G' (□), clockwise damping coefficient (○), counter-clockwise damping coefficient (●).

The reverse-flow strain profile (represented by counter-clockwise step-strain) exhibits similar step-strain profile as that in the clockwise direction. This behavior clearly shows that upon the disruption of the polymeric network, the network remains disrupted in the reverse flow deformation within the experimental time frame. This suggests that the strain-thickening behavior in the oscillating strain sweep is not due

to the re-formation of the network in the reverse flow deformation, and the cause for the oscillating strain-thickening behavior remains unclear and this provides an interesting area for future research.

4. Conclusions

The superposition of oscillation on steady shear experiment provides insights into the state of the network structure under shear deformation. With increasing applied stresses, the junction densities increased but the overall relaxation time of the system decreases. The rate of increase in the junction densities and reduction in the relaxation time determines the occurrence of shear-thinning or thickening behavior. The shear-thickening behavior corresponds to the transformation of the predominantly intra-molecular associations to inter-molecular associations. The shear-thinning behavior under moderate shear deformation is caused by the re-organization of the transient network structure. At extremely high shear stresses, this is caused by the enhanced shear-induced chain-end exit of the hydrophobes from the junction, which reduces the mechanically active chains and lifetime of the hydrophobe in a micellar junction. The strain-thickening behavior observed in oscillatory strain experiments is not caused by the bi-directional deformation. The cause for the oscillating strain-thickening behavior remains unclear and this provides an interesting area for future research.

Acknowledgements

We are grateful to Dr. David Bassett for his enthusiasm and support in this research collaboration. We would also like to acknowledge the financial support provided by the Ministry of Education of Singapore.

References

[1] Jenkins RD, Delong LM, Bassett DR. In: Glass JE, editor. Hydrophilic polymers: performance with environmental acceptability. Advances in chemical series, vol. 248. Washington, DC: American Chemical Society; 1996. p. 425.
[2] Guo L, Tam KC, Jenkins RD. Macromol Chem Phys 1998;199:1175.
[3] Dai S, Tam KC, Jenkins RD, Bassett DR. Macromolecules 2000;33:7021.
[4] Mewis J, Kaffashi B, Vermant J, Butera RJ. Macromolecules 2001;34:1376.
[5] Nagashima K, Strashko V, Macdonald PM, Jenkins RD, Bassett DR. Macromolecules 2000;33:9329.
[6] Prazeres TJV, Duhamel J, Olesen K, Shay G. J Phys Chem B 2005;109:17406.
[7] Kumacheva E, Rharbi Y, Winnik MA, Guo L, Tam KC, Jenkins RD. Langmuir 1997;13:182.
[8] (a) English RJ, Gulati HS, Jenkins RD, Khan SA. J Rheol 1997;41:427; (b) Abdala AA, Wu WJ, Olesen KR, Jenkins RD, Khan SA. J Rheol 2004;48:979.
[9] Ng WK, Tam KC, Jenkins RD. Eur Polym J 1999;35:1245.
[10] Tam KC, Farmer ML, Jenkins RD, Bassett DR. J Polym Sci Polym Phys 1998;36:2276.
[11] Tam KC, Seng WP, Jenkins RD, Bassett DR. J Polym Sci Polym Phys 2000;38:2019.
[12] (a) Horiuchi K, Rharbi Y, Spiro JG, Yekta A, Winnik MA, Jenkins RD, et al. Langmuir 1999;15:1644;
(b) Horiuchi K, Rharbi Y, Yekta A, Winnik MA, Jenkins RD, Bassett DR. Can J Chem 1998;76:1779.
[13] Iversen C, Kjoniksen AL, Nystrom B, Nakken T, Palmgren O, Tande T. Polym Bull 1997;39:747.
[14] Thuresson K, Lindman B, Nystrom B. J Phys Chem B 1997;101:6450.
[15] Petit F, Iliopoulos I, Audebert R, Szonyi S. Langmuir 1997;13:4229.
[16] Kjoniksen AL, Nystrom B, Iversen C, Nakken T, Palmgren O, Tande T. Langmuir 1997;13:4948.
[17] Tirtaatmadja V, Tam KC, Jenkins RD. AIChE J 1998;44:2756.
[18] (a) Volpert E, Selb J, Candau F. Macromolecules 1996;29:1452;
(b) Volpert E, Selb J, Candau F. Polymer 1998;39:1025.
[19] Aubry T, Moan M. J Rheol 1994;38:1681.
[20] (a) Tirtaatmadja V, Tam KC, Jenkins RD. Macromolecules 1997;30:3271;
(b) Tirtaatmadja V, Tam KC, Jenkins RD. Macromolecules 1997;30:1426.
[21] Xu B, Yekta A, Winnik MA. Langmuir 1997;13:6903.
[22] Lee KY, Jo WH, Kwon IC, Kim Y-H, Jeong SY. Macromolecules 1998;31:378.
[23] Tam KC, Jenkins RD, Winnik MA, Bassett DR. Macromolecules 1998;31:4149.
[24] Amis EJ, Hu N, Serry TAP, Hogen-Esch TE, Yassini M, Hwang FS. Associating polymers containing fluorocarbon hydrophobic units. In: Glass JE, editor. Hydrophilic polymers: performance with environmental acceptance. Advances in chemistry series, vol. 248. Washington, DC: American Society; 1998. p. 279.
[25] Sarrazin-Cartalas A, Iliopoulos I, Audebert R, Olsson U. Langmuir 1994;10:1421.
[26] Hwang FS, Hogen-Esch TE. Macromolecules 1995;28:3328.
[27] Creutz S, Stam JV, De Schryver FC, Jerome R. Macromolecules 1998;31:681.
[28] Leibler L, Rubinsetin M, Colby RH. Macromolecules 1991;24:4701.
[29] Seng WP, Tam KC, Jenkins RD. Colloids Surf A 1999;154:363.
[30] Van Den Brule BHAA, Hoogerbrugge PJ. J Non-Newtonian Fluid Mech 1995;60:303.
[31] Larson RG. In: Brenner Howard, editor. Constitutive equations for polymer melts and solution. Butterworths series in chemical engineering. Butterworth Publishers; 1988.
[32] Matsuoka S. In: Matsuoka S, editor. Relaxation phenomena in polymer. New York: Oxford University Press; 1992.
[33] Dai S, Tam KC, Jenkins RD. Macromolecules 2000;33:404.
[34] Islam MF, Jenkins RD, Bassett DR, Lau W, Ou-Yang HD. Macromolecules 2000;33:2480.
[35] (a) Sprong E, De Wet-Roos D, Tonge MP, Sanderson RD. J Polym Sci Polym Chem 2004;41:223;
(b) Sprong E, De Wet-Roos D, Tonge MP, Sanderson RD. J Polym Sci Polym Chem 2004;42:2502.
[36] Vermant J, Walker L, Moldenaers P, Mewis J. J Non-Newtonian Fluid Mech 1998;79:173.
[37] Ferry JD. Viscoelastic properties of polymers. 3rd ed. John Wiley & Sons Inc; 1980.
[38] (a) Tanaka F, Edwards SF. J Non-Newtonian Fluid Mech 1992;43:247;
(b) Tanaka F, Edwards SF. J Non-Newtonian Fluid Mech 1992;43:273.
[39] Brown EE, Burghardt WR. J Rheol 1996;40:37.